40P.

downtown

Code 1

N64-24104

CR 56548

Cat. 18

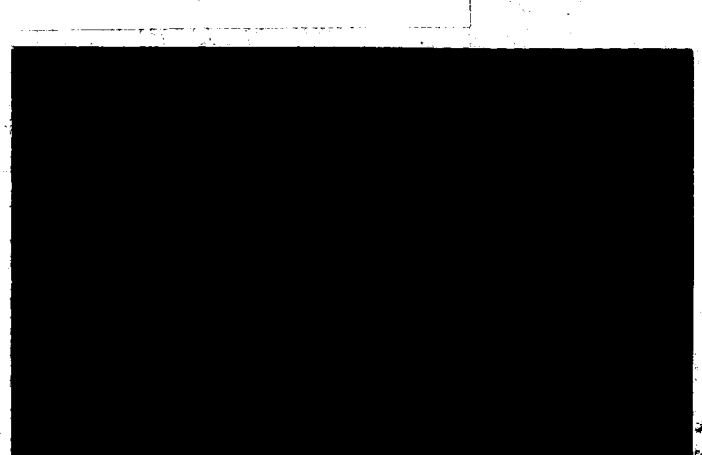

X

OTS PRICE

XEROX $ 3.60 ph

MICROFILM $ _____

D.G. Jaffstad RV-2 6/25/64

A R A, inc.

AEROSPACE RESEARCH ASSOCIATES

2017 WEST GARVEY AVENUE • WEST COVINA, CALIFORNIA • TEL. 962-1045

First Quarterly Progress Report

on

"Concepts of Multiple-Impact Study of Energy Absorption"

-2911

ARA Report
#23

1 July 1963

Reporting Period: 1 April 1963 - 1 July 1963

Principal Investigator: Bernard Mazelsky

Contract Number: NAS 7-226

Technical Status Report #1

Prepared by:

David L. Platus

Dr. David L. Platus, Project Scientist

Patrick J. Cunningham

Patrick J. Cunningham, Project Engineer

Frank A. Marovich

Frank A. Marovich, Engineer

Approved by:

Bernard Mazelsky

Bernard Mazelsky, President, ARA, Inc.

CONTENTS

LIST OF FIGURES

FIRST QUARTERLY PROGRESS REPORT
ON
"CONCEPTS OF MULTIPLE-IMPACT STUDY OF ENERGY ABSORPTION"

I. SUMMARY

24104

Flow and fatigue characteristics of ductile metals under cyclic plastic straining are summarized in relation to multiple-impact energy absorbing devices. Pertinent material parameters are identified and certain behavior trends based primarily on low-cycle-rate tests reported in the literature are discussed. From these observations idealized analytical models are developed for describing the behavior of cyclic-strain energy absorption devices utilizing metals.

An experimental program utilizing cyclic torsion tests, and aimed at extending the cyclic strain data to impact cycling conditions and verifying the analytical models, is discussed. A complete description of the test apparatus is presented. Author

II. INTRODUCTION

An attractive new concept of energy absorbing devices utilizing cyclic strain energy absorption of materials was disclosed recently by ARA, Inc. (Ref. AA). It was shown that devices of this type would be capable of specific energy absorptions (ft-lb/lb) greatly exceeding values attainable with other devices currently under study and would also be capable of multiple-impact operation. The feasibility of such devices was demonstrated at ARA, Inc. by the design, construction, and testing of an impact device utilizing cyclic plastic deformation of a copper working element (Ref. BB). The device produced a specific energy absorption in the working material approximately five times that practically attainable by unidirectional straining.

This concept of multiple-impact energy absorption has great significance in relation to space applications such as landing and docking impact devices where weight is a predominant consideration. The present research program is being conducted to study and evaluate this concept both theoretically and experimentally, and to develop improved methods for analytical prediction of the characteristics and behavior of these devices.

The characteristics and performance of cyclic strain energy-absorbing devices are directly related to the behavior of the working materials during cyclic straining. Consequently, a principal phase of this investigation involves the study of material behavior under cyclic straining conditions appropriate to energy-absorbing devices.

The scope of work for this first quarter includes a study of cyclic plastic straining of metals based primarily on low-cycle-rate tests reported in the literature; the development of idealized analytical models to describe the performance and behavior of cyclic strain energy-absorbing devices utilizing metals; and the design of cyclic torsional testing apparatus for studying metals under impact cycling conditions. Approximately 23.7% of total allotted program funds and manhours were expended during this three-month period.

III. SUMMARY OF CYCLIC PLASTIC STRAINING OF METALS IN RELATION TO ENERGY-ABSORBING DEVICES

A. Basic Concepts

The performance and behavior of energy-absorbing devices utilizing cyclic deformation of metals can be directly related to the behavior of the hysteresis

loop of the metal during cyclic straining and the relation between the hysteresis loop and fatigue life. Some of the pertinent parameters are indicated in Fig. 1. These are the total strain range, $\Delta\epsilon_T$, the plastic strain range, $\Delta\epsilon_p$, and the maximum stress range, $\Delta\sigma_{max}$. Another important parameter is the ratio of the average stress range to the maximum stress range, $\gamma \equiv \Delta\bar{\sigma}/\Delta\sigma_{max}$, which is related to the shape of the hysteresis loop.

In typical space applications such as landing impact, the total strain range will be fixed by the design. Also, the number of cycles per unit stroke length will usually be specified. Since the work done on the device per unit length of stroke is equal to the energy absorbed per cycle times the number of cycles per unit length of stroke, if friction is neglected, the resisting force during impact is directly related to the energy absorbed per cycle or the area under the hysteresis loop; i.e.,

$$F\,dx = V_w\, w_p \left(\frac{d\nu}{dx}\right) dx = (\text{const.})\, w_p\, dx,$$

or

$$F = (\text{const.})\, w_p\,, \tag{1}$$

where F is the resisting force, V_w is the volume of working material, w_p is the energy absorbed per unit volume per cycle,* $\frac{d\nu}{dx}$ is the number of cycles per unit stroke length, and dx is an increment of stroke length. Thus, the force-deflection or deceleration-time curve for the device depends on the variation of w_p with distance or time, or the variation in the area under the hysteresis loop with number

* For the present discussion it is assumed that the working material is strained uniformly.

of cycles. The behavior of the device during a particular impact depends on the variations in w_p which occur during the impact, while changes in the behavior for multiple impacts are related to changes in w_p which occur during the various impacts. Changes in w_p during a single impact depend primarily on short term effects such as temperature rise and rate sensitivity, and variations with number of impacts are related to long-term effects such as strain hardening or softening, and metal deterioration.

A second fundamental consideration in evaluating the performance of these devices is the fatigue behavior or, more specifically, the relation between the size and shape of the hysteresis curve and the number of cycles to failure. This relation governs the overall performance of the working material since it describes the total energy absorption capability, the relation between performance per impact and number of impacts possible, etc. An empirical relationship which describes the low cycle fatigue behavior of a variety of metals is given by (Ref. A),

$$N^{\frac{1}{2}} \Delta \epsilon_p = C, \tag{2}$$

where N is the total number of cycles to failure and C is a constant for the material.

The fatigue of metals from cyclic plastic straining has been studied by a number of investigators in recent years and considerable experimental data has been generated. In conjunction with these and other investigations the flow characteristics of metals during cyclic plastic straining have also been studied experimentally although available data of this type appears to be somewhat more limited. In most of these

investigations the metals were strained at very low rates and under isothermal conditions. Consequently, the data is not directly applicable to conditions of rapid cycling, as occurs during impacts where rate and temperature effects can be significant. On the other hand, considerable attention has been given to rate and temperature effects during unidirectional straining of metals. In the following sections some of the pertinent results of these studies are summarized, and general behavior trends are indicated. From these results certain behavior and performance characteristics of energy-absorbing devices are indicated and idealized models for describing their behavior are developed. In addition, areas in which further basic testing is necessary to verify and improve these models are discussed.

B. Flow Characteristics of Metals under Cyclic Straining

The flow characteristics or stress-strain behavior of ductile metals under cyclic plastic straining have been studied by a number of investigators. Although most of the test data have been generated under very low cycling rates where rate and temperature effects are not significant, some general behavior trends have been observed which are pertinent to energy-absorbing devices. Some of these are briefly reviewed.

One of the most significant of these observations is the pronounced Bauschinger effect which is operable in most ductile metals under completely reversed cyclic plastic straining. In the absence of this effect the flow characteristics or strain-hardening behavior of metals under cyclic straining conditions might be estimated from the classical theory of plasticity. According to this theory the state of strain-hardening of a ductile metal depends on the total plastic strain imposed or plastic work done on

the metal, and the actual functional relation between stress and strain can be determined from a tensile test. However, in the case of completely reversed cyclic straining of ductile metals the strain-hardening behavior departs radically from the classical plastic behavior. Rather than hardening with plastic strain according to the tensile curve, the data from a number of investigators indicates that strain hardening (or softening) develops in the first few cycles, after which further cycling causes hardening or softening at a rather slow rate. Moreover, the maximum stress to which the material hardens, or the "saturation" stress, depends on the plastic strain range, $\Delta \epsilon_p$. In general, the higher the value of $\Delta \epsilon_p$, the more rapid is the strain-hardening and the higher the "saturation" stress.

Typical stress-strain behavior of a ductile metal during strain cycling might be as indicated qualitatively in Fig. 2. The rate and extent of strain-hardening depends on the total strain range, as shown in the figure. The stress range at "saturation" increases with strain range, as mentioned above. Quantitative examples of this effect are given in Figs. 3 to 7. Fig. 3, based on the data of Ref. 8, shows the increase in stress with number of cycles for cyclic straining of 24 ST aluminum alloy at various plastic strain ranges.* Because of the large strain ranges "saturation" occurred very quickly. From the results of Fig. 3 a curve of "saturation" stress vs. strain range has been constructed and is shown in Fig. 4. Also shown in this figure is the initial true stress-strain curve for the material. Curves of this type are useful in the design and analysis of energy-absorbing devices since they indicate the resisting stress and the

* In most of these tests the elastic range was small compared with the total strain range so that $\Delta \epsilon_p \simeq \Delta \epsilon_T$.

performance of the device vs. strain range, after the hysteresis loop has been developed. Moreover, it is of interest to seek a general relation between the "saturation" stress vs. strain range and the initial stress-strain curves for typical ductile metals. Such a relation would permit the evaluation and comparison of a variety of metals from their tensile data, which is much more readily attainable than data on cyclic straining behavior.

Although typical data indicate that ductile metals strain-harden during initial development of the hysteresis loop, some data show an initial strain-softening as well. In general, annealed metals appear to strain-harden while hardened or cold-worked metals appear to strain-soften. Figs. 5 and 6 show these effects for hard and soft copper and steel, based on the data of Ref. C. Here, stress amplitude ($\Delta\sigma_{max}/2$) is plotted against total plastic strain ($2N\Delta\epsilon_p$) for different values of total strain range. It appears, from these data, that strain-softening of the cold-worked metals takes place more slowly than strain-hardening of the annealed metals. Further examples of strain-hardening and strain-softening are shown in Fig. 7, based on the data of Ref. D.

It is apparent from Fig. 2 that the shape of the hysteresis loop, as described by the parameter ζ, or the ratio of average to maximum stress ranges, is an important factor in the evaluation of energy-absorbing devices. Since, from the defining relation for ζ,

$$w_p = \int_{\substack{\text{hysteresis}\\ \text{loop}}} \sigma d\epsilon_p \equiv \zeta \Delta\sigma_{max} \Delta\epsilon_p, \qquad (3)$$

w_p is directly proportional to ζ for fixed values of $\Delta\sigma_{max}$ and $\Delta\epsilon_p$.

Thus, variations in w_p and in the deceleration-time behavior of these devices could result from variations in γ, even if $\Delta\sigma_{max}$ and $\Delta\epsilon_p$ remained fixed. Typical data on flow characteristics of ductile metals under cyclic straining indicate that strain-hardening during the tensile and compressive parts of the hysteresis loop decreases with increasing strain range. I.e., γ increases with increasing strain range. Moreover, the data further indicate that the shape as well as the size of the loop develops during the first few cycles and changes very slowly with increased cycling. However, most of the available data were generated under low rate and nearly isothermal conditions. Thus, for application to impact cycling conditions, it is important to evaluate the effects of high cycling rates and temperature rise on γ, and their consequent effects on the performance of the devices.

IV. EFFECTS OF FLOW CHARACTERISTICS ON PERFORMANCE

A. Basic Considerations

From the foregoing discussion it is apparent that various changes in the flow characteristics of the working metal during strain cycling can affect the performance and behavior of an energy-absorbing device. Thus, under different design conditions, three different force-deflection or deceleration-time curves for a device might result, as indicated in Fig. 8. Curve A, which might represent the optimum for such a device, could result for the case where the hysteresis loop were established and did not change with cycling during the impact; or, it could result for a case where the hysteresis loop changed but in such a way that the area under the loop remained constant. Curves B and C could result for cases in which the area under the hysteresis loop increased or decreased, respectively, during impact.

From the previous discussion of flow characteristics of metals during cycling, it becomes apparent that an increase in flow stress alone can increase or decrease the area under the hysteresis loop, depending on other parameters of the loop. This is illustrated in Fig. 9. Fig. 9a represents a case where $\Delta\epsilon_p$ is small compared with $\Delta\epsilon_T$, i.e., a case where a large number of impacts or a large number of cycles to failure is required. The solid curve represents the hysteresis loop at the start of cycling and the dotted curve represents the loop after an increase in flow stress. It is seen that the increase in stress is more than compensated for by the decrease in $\Delta\epsilon_p$, for a constant value of $\Delta\epsilon_T$, so that the net result is a decrease in w_p. Fig. 9b, on the other hand, represents a case where $\Delta\epsilon_p$ is almost equal to $\Delta\epsilon_T$, and would result if only a small number of cycles to failure were required. Here it can be seen that an increase in stress results in an increase in w_p.

For cases where the elastic strain range, $\Delta\epsilon_E$, is important, such as in Fig. 9a, it is convenient to make use of the relations

$$\Delta\epsilon_T = \Delta\epsilon_p + \Delta\epsilon_E, \tag{4}$$

and

$$\Delta\epsilon_E = \frac{\Delta\sigma_{max}}{E}, \tag{5}$$

and to rewrite Eq. (3) in the form,

$$w_p = \gamma\Delta\sigma_{max}\left(\Delta\epsilon_T - \frac{\Delta\sigma_{max}}{E}\right). \tag{6}$$

From Eq. (6) it is possible to estimate the effect of a change in $\Delta\sigma_{max}$ on w_p. Assuming that γ, $\Delta\epsilon_T$, and E remain constant,

$$\frac{dw_p}{d\Delta\sigma_{max}} = \gamma\left(\Delta\epsilon_T - 2\frac{\Delta\sigma_{max}}{E}\right). \tag{7}$$

Thus, for the condition where a change in $\Delta\sigma_{max}$ causes no change in w_p, $\frac{dw_p}{d\Delta\sigma_{max}}$ is zero, and Eq. (7) gives

$$\Delta\epsilon_T = 2\frac{\Delta\sigma_{max}}{E}. \tag{8}$$

By Eqs. (4) and (5) it is seen that this corresponds to $\Delta\epsilon_p = \Delta\epsilon_E$. Thus, for $\Delta\epsilon_p < \Delta\epsilon_E$, an increase in $\Delta\sigma_{max}$ during an impact results in a decrease in w_p, which gives rise to a load-deflection curve of type C in Fig. 8; conversely, a decrease in $\Delta\sigma_{max}$ results in an increase in w_p and a curve of type B. Similarly, for $\Delta\epsilon_p > \Delta\epsilon_E$, an increase in $\Delta\sigma_{max}$ during impact results in a curve of type B and a decrease in $\Delta\sigma_{max}$ results in a curve of type C.

The "cross-over" value of strain range given by Eq. (8) is of interest since, within the limitations of the foregoing assumptions, it corresponds to a hysteresis loop relatively insensitive to changes in $\Delta\sigma_{max}$, and a load-deflection curve of type A in Fig. 8. A typical value can be estimated for 24 ST aluminum alloy, using the curves of Fig. 4 and a value for E of 10.6×10^6 psi. Taking a value of twice the "saturation" stress for $\Delta\sigma_{max}$ equal to 100,000 psi, the "cross-over" value

for $\Delta\epsilon_T$ is about two percent and $\Delta\epsilon_p$ is about one percent. With a value for C in Eq. (2) of 0.48, from Ref. A, the number of cycles to failure for this case is 23,000. Thus, for a typical landing impact device using 24 ST aluminum alloy, which produces perhaps 20 cycles per impact, the "cross-over" condition would correspond to a capability of about 1200 impacts.

B. Temperature and Rate Effects

Two effects which could produce changes in flow stress during an impact are temperature rise and variation in rate of straining. However, if rate-sensitivity effects are of the same order of magnitude for cyclic plastic straining as they are for unidirectional straining, the result of these effects should be small for most cases of interest. This is demonstrated by the following example.

Rate sensitivity, n, is defined by

$$n = \left(\frac{\partial \ln \sigma}{\partial \ln \dot{\epsilon}_p} \right)_{\epsilon_p}, \tag{9}$$

where σ is the flow stress corresponding to a particular value of ϵ_p and $\dot{\epsilon}_p$ denotes the derivative of ϵ_p with respect to time. This equation is normally used to relate changes in flow stress with changes in uniform strain rate during unidirectional straining. Thus, in the range where Eq. (9) is applicable,

$$\sigma \sim \dot{\epsilon}_p^{\,n}, \tag{10}$$

for a given plastic strain, or,

$$n = \frac{\ln \sigma_2/\sigma_1}{\ln \dot{\epsilon}_{p_2}/\dot{\epsilon}_{p_1}} \tag{11}$$

where the subscripts denote two different strain rates. Rate sensitivity values at room temperature are usually in the neighborhood of 0.01, and those at elevated temperatures are in the neighborhood of 0.1.*

For the present example, it is assumed that the strain is applied sinusoidally and that the elastic strain range is negligible so that $\Delta \epsilon_p \simeq \Delta \epsilon_T$. Thus,

$$\epsilon_p = \frac{\Delta \epsilon_p}{2} \sin \omega t \ , \tag{12}$$

and

$$\dot{\epsilon}_p = \frac{\omega \Delta \epsilon_p}{2} \cos \omega t \ , \tag{13}$$

where ω is the cycling frequency and is related to ν by

$$\omega = \frac{1}{2\pi} \frac{d\nu}{dt} \ . \tag{14}$$

Sinusoidal straining in actual tests gives rise to hysteresis loops of the type previously discussed, as illustrated in Fig. 10. Thus, if rate sensitivity effects during cyclic

* See, for example, Ref. E, pp. 171-195.

straining are similar to those for unidirectional straining, it might be expected that the maximum stress range at "saturation" would be proportional to the amplitude of $\dot{\epsilon}_p$, or, by Eqs. (10) and (13),

$$\Delta \sigma_{max} \sim \omega^n \tag{15}$$

Consider the effect of rate sensitivity on an impact device in which the onset velocity v_o corresponds to a cycling frequency ω_o, i.e.,

$$v = \frac{dx}{dt} = \frac{dx}{dv}\frac{dv}{dt} = 2\pi\left(\frac{dx}{dv}\right)\omega \ , \tag{16}$$

or,

$$v = (\text{const.})\ \omega \quad \text{and} \quad v_o = (\text{const.})\ \omega_o \ , \tag{17}$$

provided $\frac{dx}{dv}$ is constant.

By Eqs. (1), (6), (15) and (17),

$$\frac{F}{F_o} = \left(\frac{\omega_p}{\omega_{p_o}}\right)^n = \left(\frac{\Delta\sigma_{max}}{\Delta\sigma_{max_o}}\right)^n = \left(\frac{v}{v_o}\right)^n \ , \tag{18}$$

assuming, as before, that η and $\Delta\epsilon_T$ are constant. Here the subscript o denotes a quantity corresponding to the onset velocity. Thus, as the velocity decreases during impact rate sensitivity effects give rise to a load-deflection curve of type C in Fig. 8. If it is assumed that the effects are small so that the force and deceleration are effectively constant,

$$v^2 = v_o^2 + 2ax \tag{19}$$

and

$$\left(\frac{v}{v_o}\right)^2 = 1 - \frac{x}{L} \tag{20}$$

where L is the total stroke length and $-a$ is the deceleration. From Eqs. (18) and (20), the load-deflection relation can be written

$$\frac{F}{F_o} = \left(1 - \frac{x}{L}\right)^{n/2} \tag{21}$$

Assuming, for example, a rate sensitivity of 0.02, the value of $\frac{F}{F_o}$ at $x/L = 0.5$ would be 0.993. Thus, for typical room temperature rate sensitivity values in the neighborhood of 0.01 this effect would be negligible and the load-deflection curve would be essentially flat. Even for cases where the metal increased in temperature so that the rate sensitivity increased, the effect on the load-deflection behavior should be small, provided, of course, that rate effects for cyclic straining are of the same order of magnitude as for unidirectional straining.

For cases where the metal temperature increases appreciably a more significant effect on load-deflection behavior than rate sensitivity will probably be the decrease in flow stress due to the temperature rise. For some ductile metals, the change in flow stress during unidirectional straining can be described by a relation which has the form

$$\frac{\sigma}{\sigma_o} = \exp\left[K\left(\frac{1}{T} - \frac{1}{T_o}\right)\right], \tag{22}$$

where K is a constant for the material, T is the absolute temperature, and the subscript o refers to some reference temperature. This relation is generally used to describe the effect of temperature on flow stress for a particular strain and strain rate, and the parameter K can be estimated, for example, from tensile strength data. Moreover, the extension of such a relation to cases of variable temperature and strain rate histories requires the postulate of a "mechanical-equation-of-state" concept which ignores temperature and rate history effects. Although there exists evidence that such a concept is generally invalid, the errors resulting for many load histories are sufficiently small that the concept can be used as a first approximation.* Furthermore, the validity of extending this concept to describe saturation flow stress behavior during cyclic plastic straining has not been verified. However, if it is assumed that the maximum stress range during strain cycling is affected by temperature according to Eq. (22), the resulting effect on load-deflection behavior can be estimated.

Assuming, as before, that the elastic strain range is negligible and that $d\nu/dx$, η, and $\Delta\epsilon_T$ are constant, Eqs. (1), (6) and (22) yield

$$F(x) = F_o \exp\left[-K\left(\frac{1}{T_o} - \frac{1}{T(x)}\right)\right] , \qquad (23)$$

where the reference state corresponds to the initial temperature of the metal. The

* See, for example, Ref. E, Chap. 7.

temperature rise is equal to the plastic work done on the metal, provided friction is neglected, so that

$$\frac{dT}{dx} = \frac{F(x)}{M_w c} \quad , \tag{24}$$

where M_w is the mass and c is the heat capacity of the working metal. Combination and integration of Eqs. (23) and (24) yield the result,

$$T e^{-\frac{K}{T}} - K\left[E_i\left(\frac{-K}{T_o}\right) - E_i\left(\frac{-K}{T}\right)\right] = \left(\frac{F_o}{M_w c} x + T_o\right) e^{-\frac{K}{T_o}} \quad , \tag{25}$$

where Ei is the exponential integral, defined by*

$$E_i(t) \equiv \int_{-\infty}^{t} \frac{e^{\tau}}{\tau} d\tau \quad , \tag{26}$$

and which can also be expressed in series form by

$$E_i(t) = -\ln t - \gamma + t - \frac{t^2}{2 \cdot 2!} + \frac{t^3}{3 \cdot 3!} - \frac{t^4}{4 \cdot 4!} + \cdots \quad , \tag{27}$$

where $\gamma = 0.5772$. Eq. (25) can be solved for different values of T to yield a curve of x vs. T. Substitution of these values in Eq. (23) then yields the required load-deflection curve.

* See, for example, Ref. F, p. 96.

An example is shown for an impact device utilizing 347 SS working metal, which is designed to produce a specific energy absorption in the working metal of 84,000 ft-lb/lb during a single impact. Assuming adiabatic conditions, this produces a 900° F temperature rise during the impact and a decreasing load-deflection curve. Assuming an initial temperature of 70° F, the value of K for 347 SS in this range, based on tensile strength data, is 347° F. With these values, Eqs. (23) and (25) yield the load-deflection curve shown in Fig. 11.

V. TEST PROGRAM

A. Objective

A test program is currently underway to study cyclic straining of metals under conditions appropriate to impact devices and its application to actual devices.

Phase I of this program consists of a basic experimental study of flow and fatigue characteristics under rapid cycling rates where rate sensitivity and temperature effects can be significant. A principal objective of this phase is to evaluate and compare flow and fatigue characteristics of several promising ductile metals with similar data obtained under low cycling rates, and to compare cyclic flow characteristics with those obtained under unidirectional straining. In addition, an attempt will be made to evaluate and compare rate sensitivity and temperature effects with similar unidirectional data.

Phase II of this program will include the design, construction, and testing of an impact device utilizing a metal torus element. This phase will provide a means of testing the analytical models developed for predicting the behavior of such devices, utilizing data of the type generated in Phase I.

For the Phase I studies, it was decided to utilize cyclic torsion tests with tubular specimens. In this manner it is possible to study flow characteristics under approximately uniform states of deformation and stress. The metals selected are 347 stainless steel, 24 ST aluminum alloy, and molybdenum. The 347 SS and 24 ST aluminum were selected on the basis of their specific energy absorption capabilities and availability of low cycle rate test data, and the molybdenum was selected because of its unique temperature capabilities and their consequent effect on specific energy absorption.

The pertinent parameters to be varied during the test are total strain range, cycling rate, temperature, and duration of run. The latter parameter, analogous to number of cycles per impact, controls the temperature rise of the specimen during a run. The resisting torque, from which flow stress can be computed, will be monitored continuously throughout a run. It is also planned to measure fatigue life for the various cycling conditions. A complete description of the test apparatus is presented in the following section.

B. Cyclic Torsion Test Apparatus

This apparatus is designed to apply cyclic strain to a series of torsion specimens. The apparatus is schematically outlined in Fig. 12. The measurements to be recorded were described in the previous section under Phase I; briefly, they are: strain range, cyclic rate, total cycles, strain torque, and temperature history.

Certain parameters are built into the device and are not directly measured. The total strain range is set by the adjustment of a cam mechanism (8)

which drives a gear. This determines the angular oscillating motion of torsional strain applied to the moving end of the specimen (10). The cyclic rate is varied over and under the motor drive rate by means of a pulley combination (6) between the clutch shaft and the cam shaft. The drive rate of the motor (3) is approximately 50 cps and is adjustable to 25 cps or 100 cps. A large fly wheel (4) attached to the motor shaft will provide essentially constant rate for short runs of 5 to 20 cycles. The actual number of cycles from initial start to shutdown will be predetermined by a preset subtraction counter (7) and this counter will also measure the total complete cycles for each run. A clutch control unit (2) connects the drive cam to the motor and the engagement can be varied to control the acceleration forces.

An oscillograph recorder (14) and amplifier control unit (13) will be used to record the torque (strain force), cyclic variations, temperature rise, and total cycles per run. The oscillograph record will have a precision time pulse record as part of each run. This record will provide time base for reduction of the recorded data. The strain history of each cycle will be generated by a strain gage load cell (12) which will convert the torque into electrical signals to be recorded by the oscillograph. In this record will be the torque history of each cycle, the total cycles, and the cyclic rate for each run. The counter will be used to total the actual number of cycles required at failure. If possible, a thermal record will be obtained on a channel of the oscillograph for each run. The exact technique for temperature recording has not been determined at the writing of this report.

The specimen is designed to permit a strain range from zero through the elastic to include approximately 10 percent plastic (Fig. 13). Adjustments of the torque arm and the cam drive will allow adequate electrical outputs for all of the tests presently programmed. Twenty specimens of each of three materials are scheduled for testing over a variation of rates and strain ranges. The number of cycles per run will be determined by the temperature rise during each run. As an example, the stainless steel specimen at 100 cps and 5% strain can be expected to heat itself approximately 1000° F in less than 10 strain cycles. The number of cycles per run will be limited to the range of 5 up to 100 except for special tests whose heating effects are to be observed. A few runs with the specimen preheated to a scheduled temperature are proposed, depending upon the test time available.

VI. FUTURE WORK

The purpose of this section is to describe briefly the anticipated work that will be required during the next quarterly period. Emphasis will be placed on obtaining adequate experimental data, analysis thereof as well as correlation of the analytical models required for their verification. Finally, the basic data should then be used for prediction of performance for actual impact devices. Detailed outlined of this future work is provided as follows:

A. The complete apparatus described in Section V, Test Program, will be calibrated to insure proper interpretation of results.

B. Preliminary trial runs of the apparatus will be performed during this period for possible debugging of the mechanical systems involved.

C. Complete cyclic torsion tests will be made on the following three metals:

1. 24 ST aluminum
2. Type 347 stainless steel
3. Molybdenum

D. Correlation of the rapid cyclic strain behavior with flow rate behavior which has been described in the literature will be made. If discrepancies exist, possible explanations will be evaluated.

E. As a result of the test described in "C", an attempt will be made to evaluate rate sensitivity and temperature effects.

F. Previous analytical models described in both the literature and the work conducted under this study contract will be verified.

G. An attempt will be made to apply the basic data obtained in the described test program, Section V, to predict the performance and behavior of actual impact devices.

Although all of the previous items may not be obtained during the next quarter, every attempt will be made to obtain adequate data. Should problems arise, these will be reported in the Monthly Status Reports.

FIGURE 1. HYSTERESIS LOOP

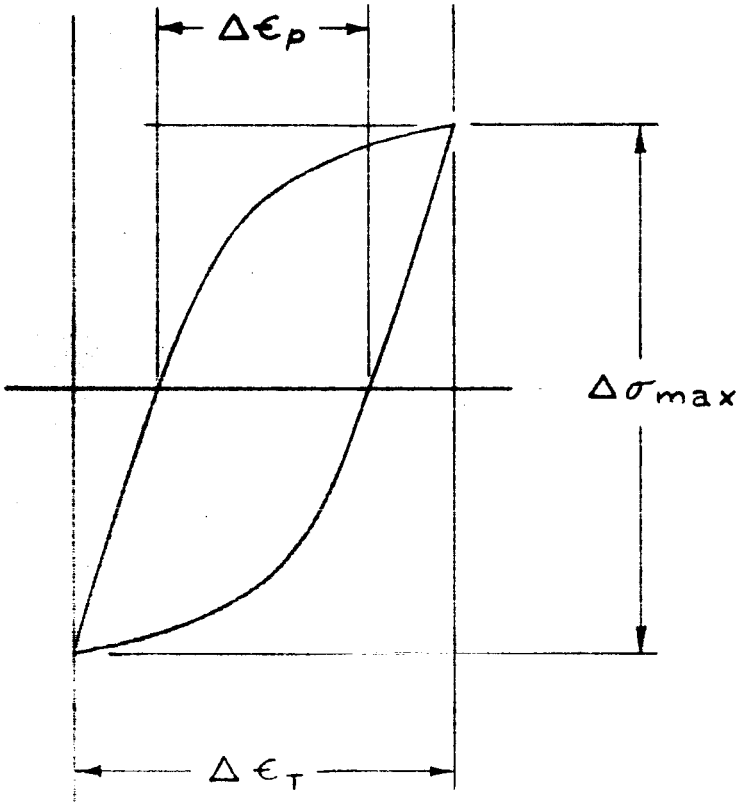

FIGURE 2 EFFECT OF TOTAL STRAIN RANGE ON HYSTERESIS LOOP

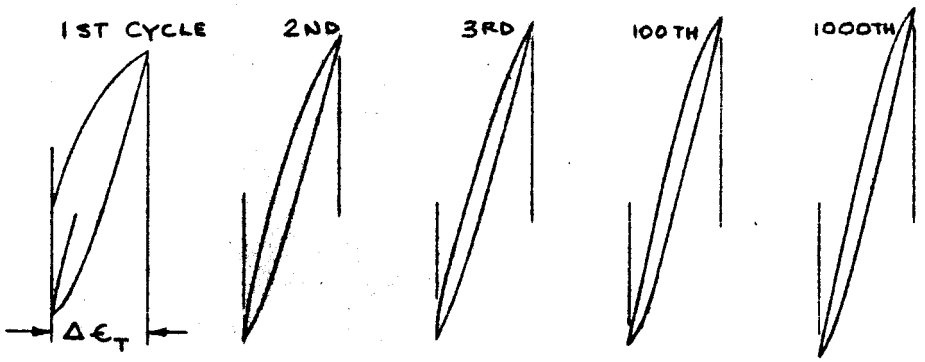

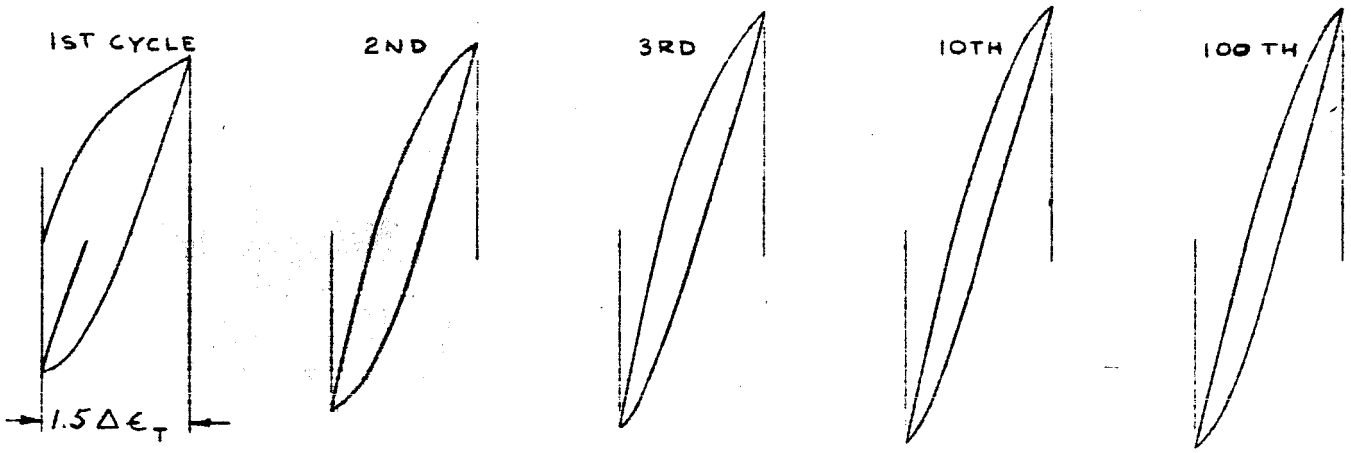

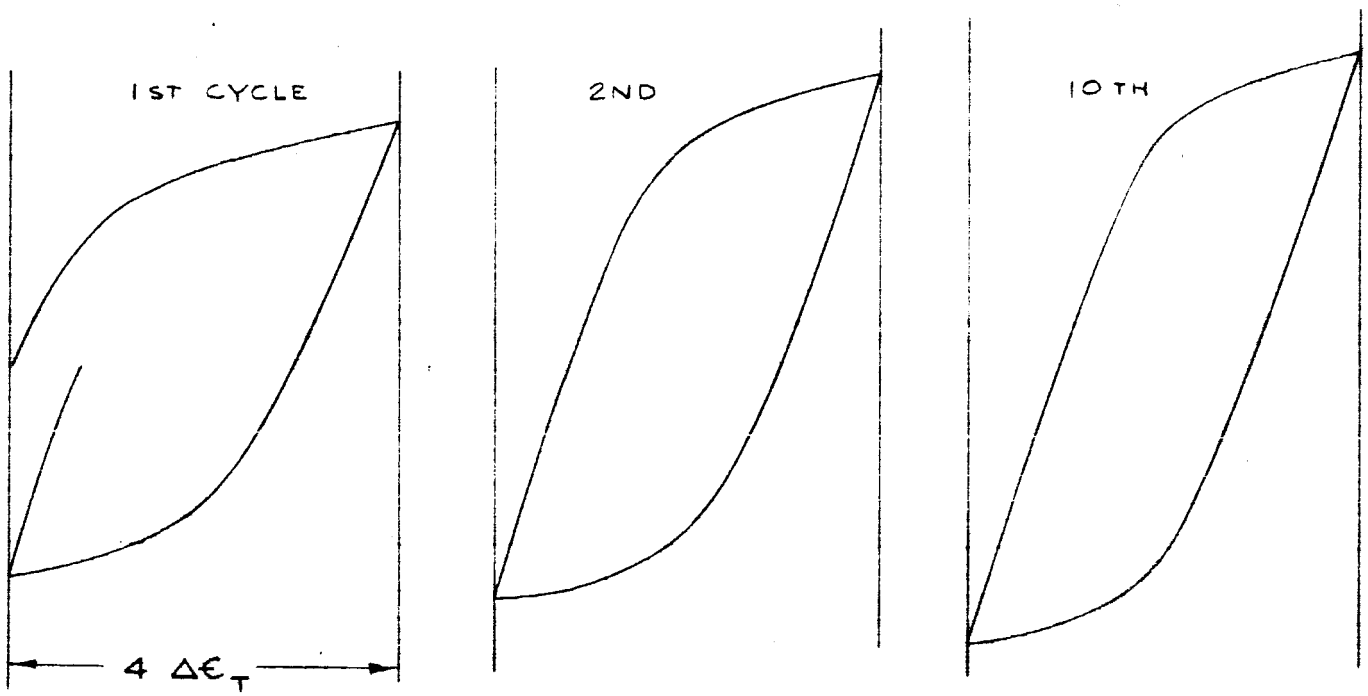

FIGURE 3. CHANGE IN APPLIED STRESS FOR CYCLIC STRAINING OF 24 ST ALUMINUM ALLOY ROD

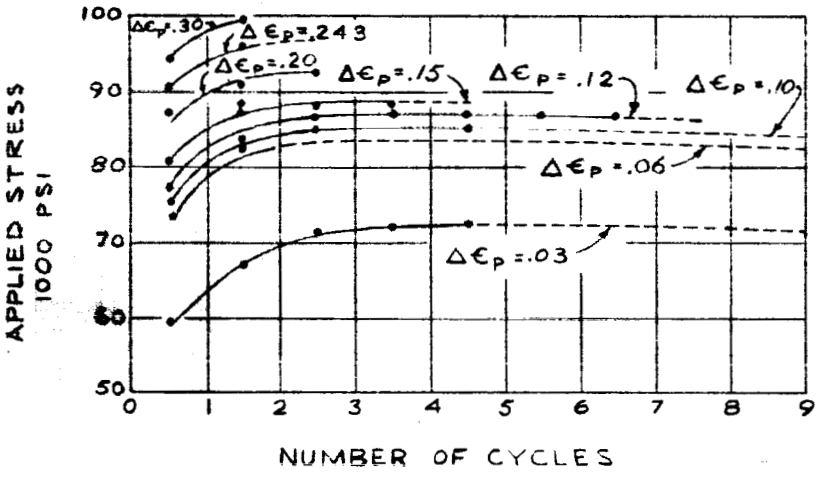

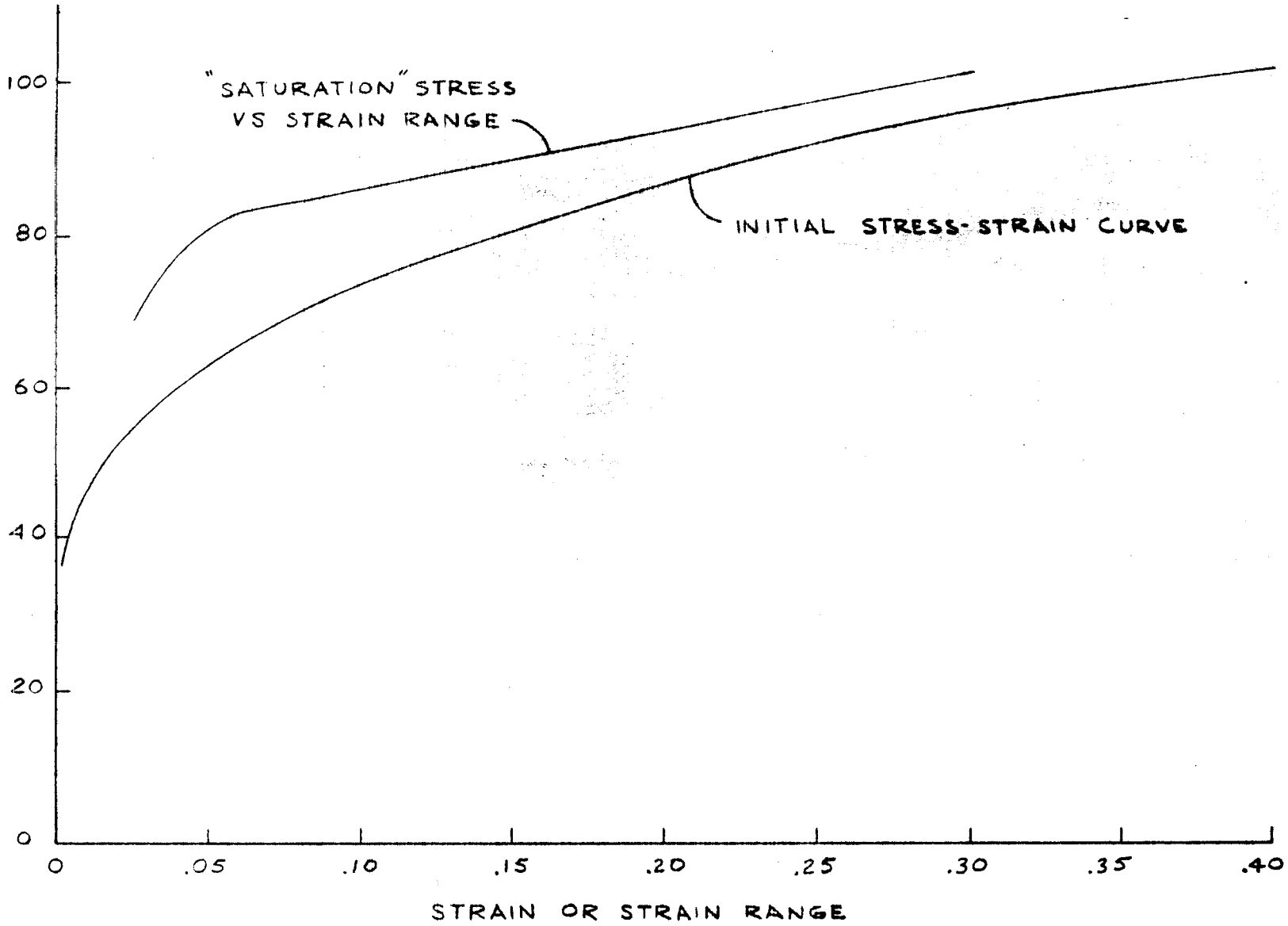

FIGURE 4. EFFECT OF STRAIN RANGE ON "SATURATION" STRESS FOR 24 ST ALUMINUM ALLOY ROD

FIGURE 5. HARDENING AND SOFTENING OF SOFT AND HARD COPPER BY CYCLIC PLASTIC STRAINING

a. SOFT COPPER

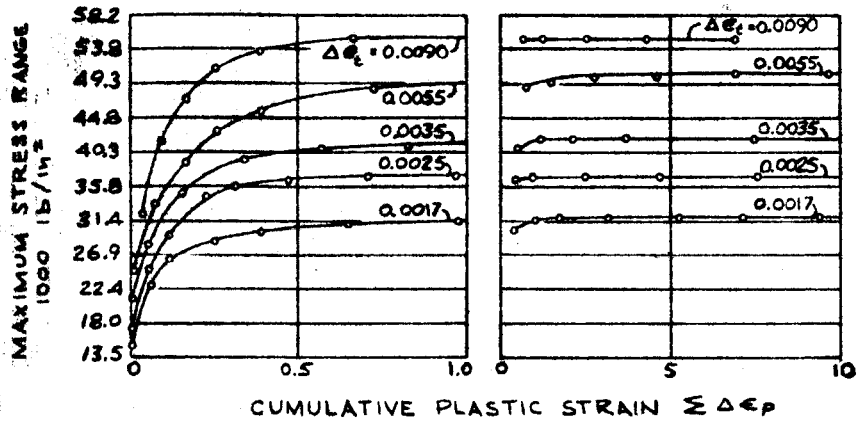

b. HARD COPPER

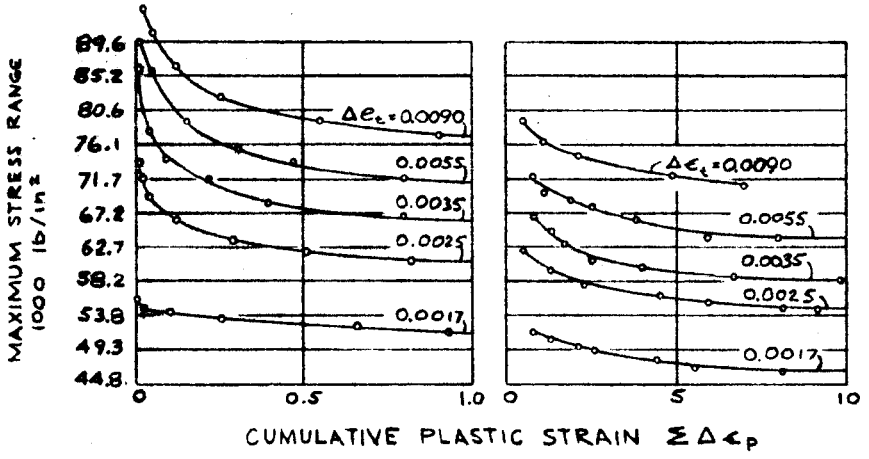

FIGURE 6. HARDENING AND SOFTENING OF SOFT AND HARD STEEL BY CYCLIC PLASTIC STRAINING

a. SOFT STEEL

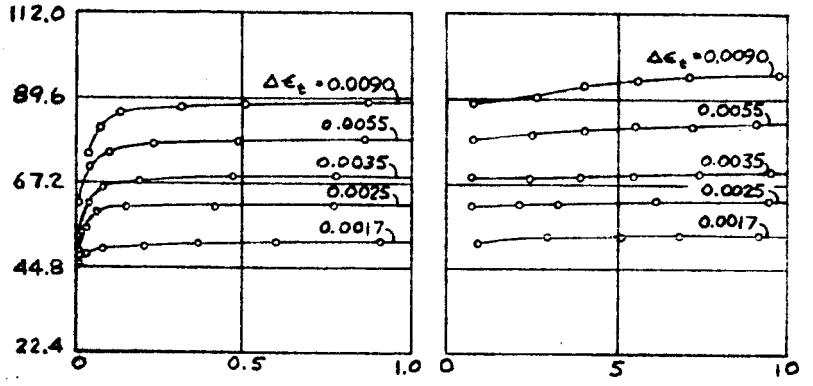

b. HARD STEEL

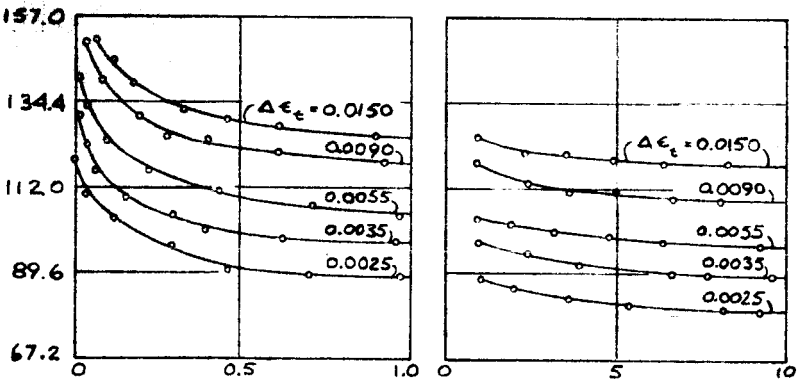

FIGURE 7. VARIATION OF LOAD WITH NUMBER OF STRAIN CYCLES

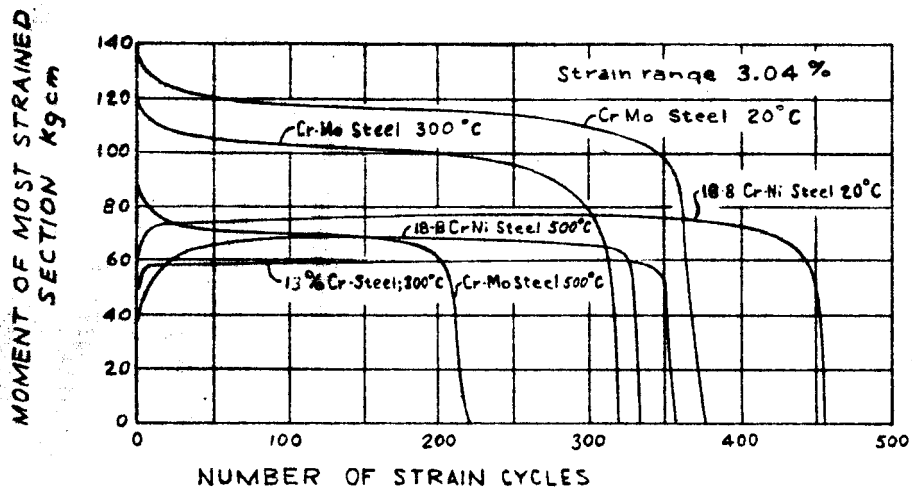

FIG. 8. TYPICAL LOAD - DEFLECTION OR DECELERATION—TIME BEHAVIOR:

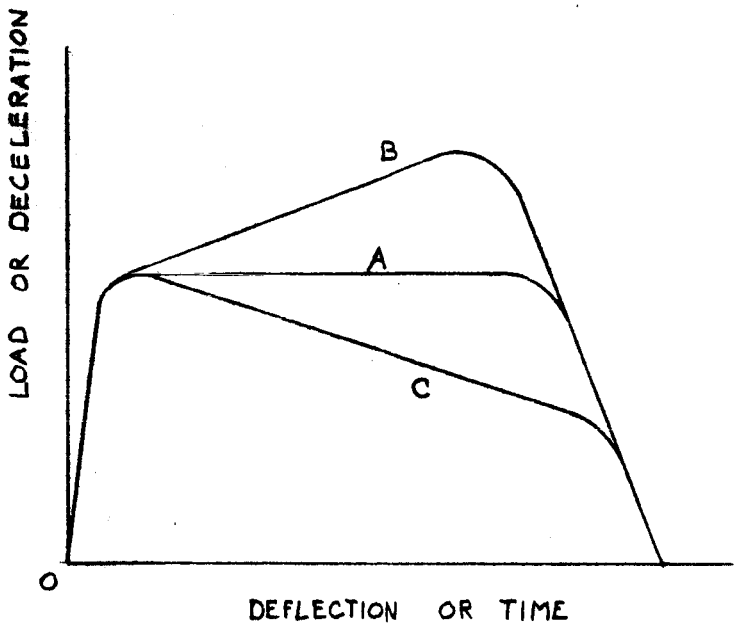

FIGURE 9 EFFECT OF INCREASE IN FLOW STRESS ON HYSTERESIS LOOP

(a) $\Delta\epsilon_p$ SMALL COMPARED WITH $\Delta\epsilon_T$

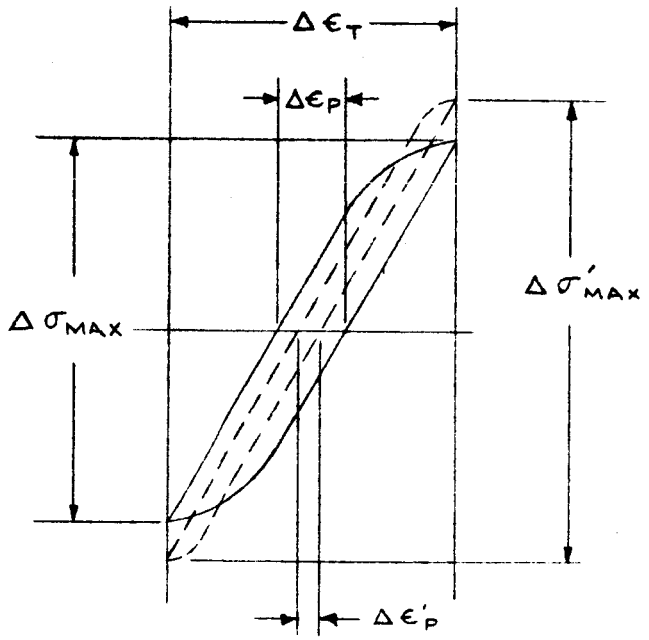

$\omega_p' < \omega_p$

(b) $\Delta\epsilon_p$ ALMOST EQUAL TO $\Delta\epsilon_T$

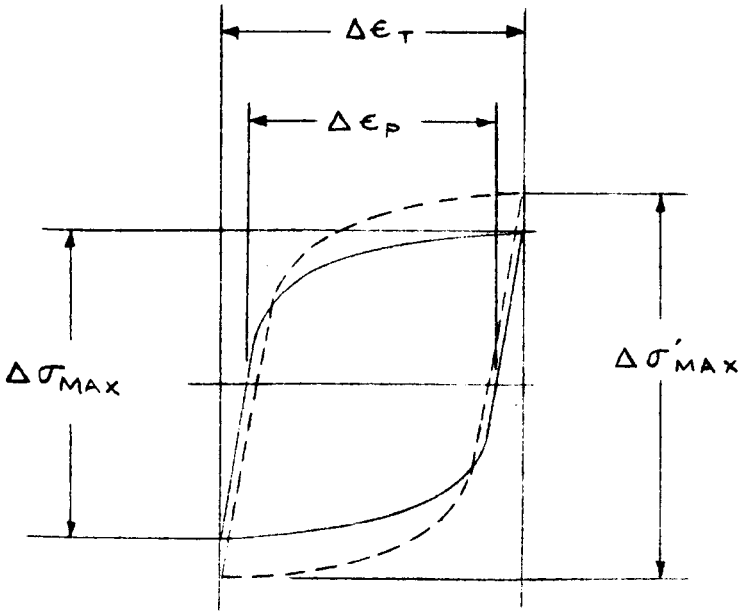

$\omega_p' > \omega_p$

FIG 10. RELATION BETWEEN STRESS, STRAIN, AND TIME DURING SINUSOIDAL STRAINING

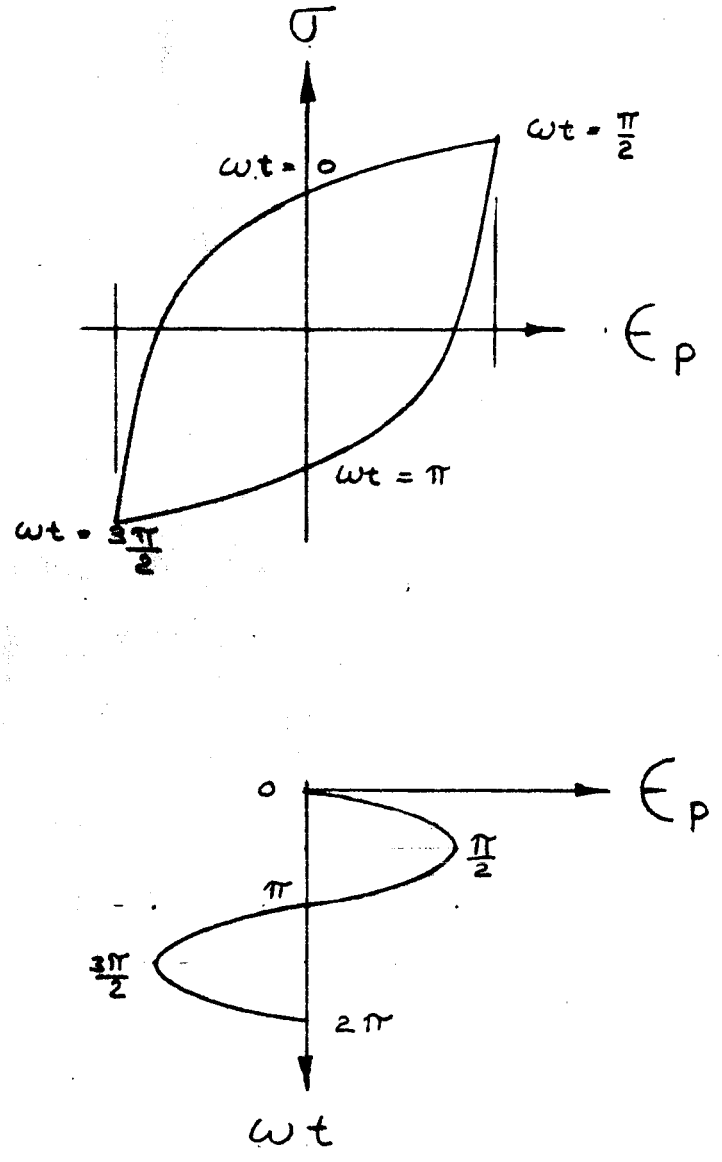

FIG 11. LOAD - DEFLECTION CURVE FOR IMPACT DEVICE UTILIZING 347 STAINLESS STEEL ELEMENTS. (IMPACT PRODUCES 900°F TEMPERATURE RISE)

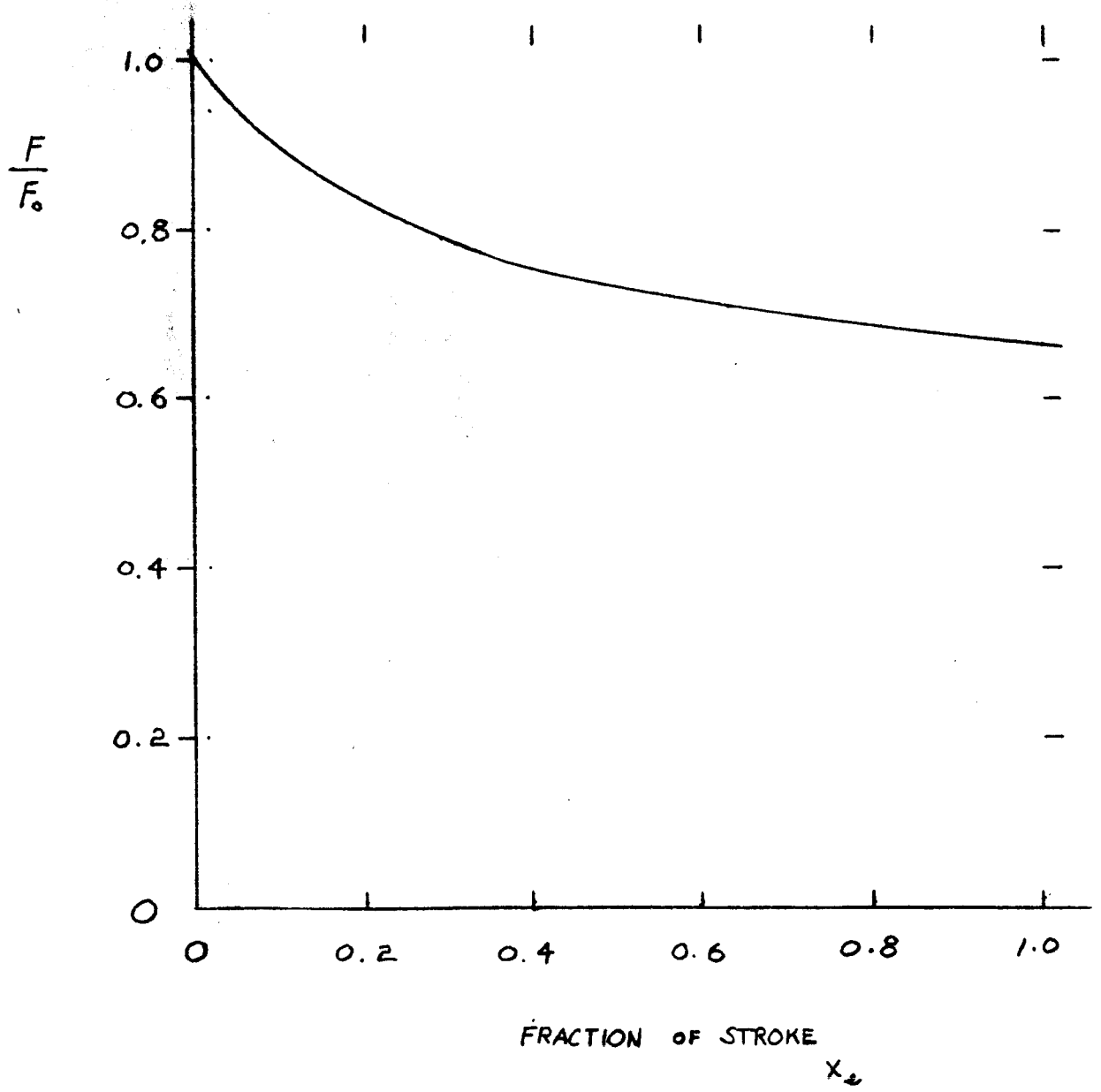

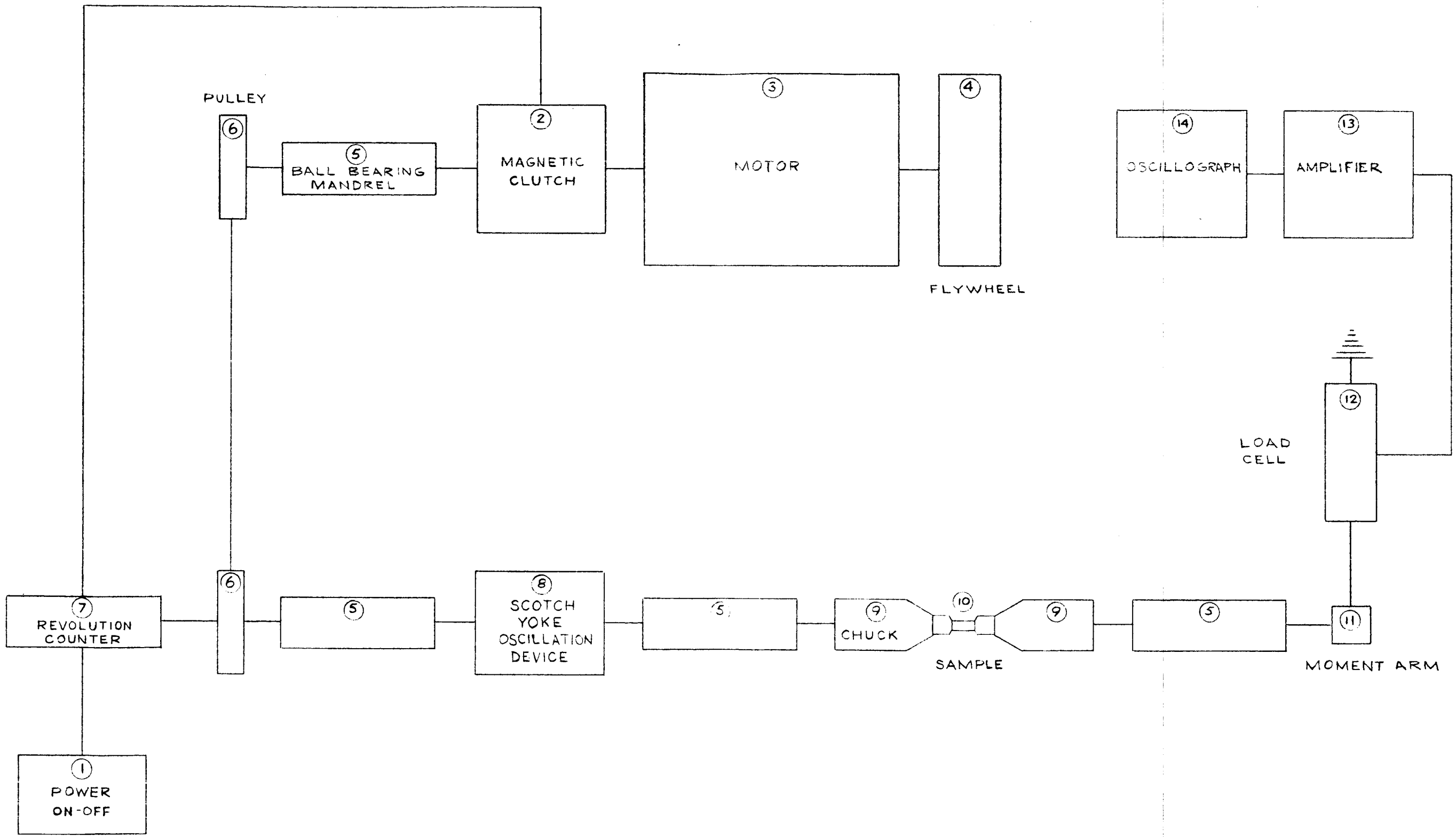

FIGURE 12. SCHEMATIC, CYCLIC TORSION TEST APPARATUS

FIG 13. TEST SPECIMEN.

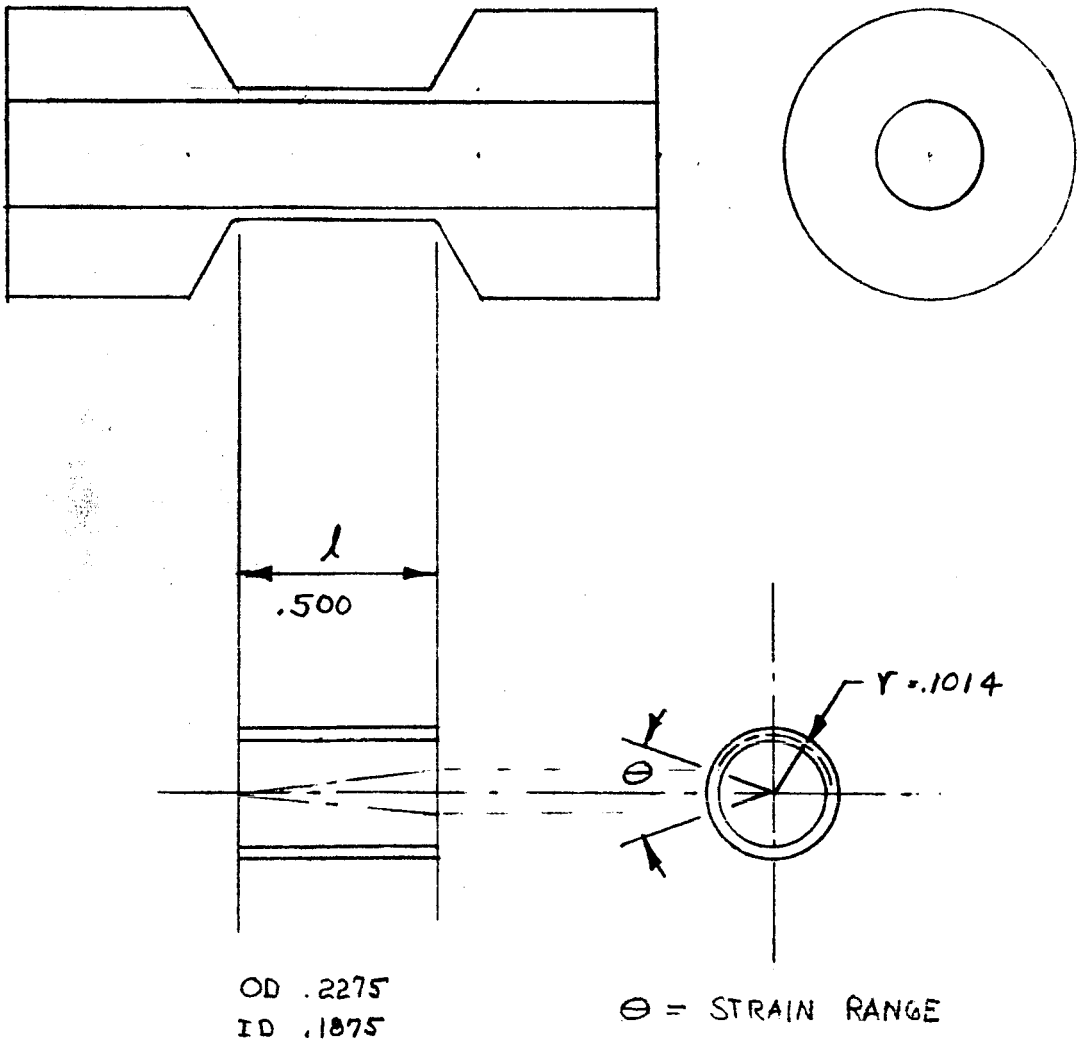

OD .2275
ID .1875

θ = STRAIN RANGE

REFERENCES

AA. D. L. Platus and F. A. Marovich. An Invention for Multiple-Impact High Energy-Absorbing Devices Utilizing Cyclic Deformation of Metals, ARA Report #9, 18 December 1962.

BB. D. L. Platus. A Reduction to Practice of a Multiple-Impact High Energy-Absorbing Device Utilizing Cyclic Deformation of a Metal, ARA Report #16, 30 March 1963.

A. J. F. Tavernelli and L. F. Coffin, Jr., "A Compilation and Interpretation of Cyclic Strain Fatigue Tests on Metals," Transactions, American Society for Metals, Vol. 51, 1959, pp. 438-453.

B. S. I. Liu, G. Sachs, J. J. Lynch, and E. J. Ripling, "Low Cycle Fatigue of the Aluminum Alloy 24 ST in Direct Stress," Trans. AIME, Vol. 175 (1948B), p. 469.

C. D. S. Dugdale, "Stress-Strain Cycles of Large Amplitude," Journal of the Mechanics and Physics of Solids, Vol. 7, 1959, pp. 135-142.

D. A. Johansson, "Fatigue of Steels at Constant Strain Amplitude and Elevated Temperatures," Proceedings, Colloqium on Fatigue, Stockholm, 1955.

E. J. D. Lubahn and R. P. Felgar. Plasticity and Creep of Metals. New York: John Wiley & Sons, Inc., 1961.

F. B. O. Pierce and R. M. Foster. A Short Table of Integrals, Fourth Edition. Boston: Ginn and Company, 1956.

G. L. F. Coffin, Jr., "A Study of the Effects of Cyclic Thermal Stresses in Ductile Metals," Transactions, ASME, Vol. 76, 1954, pp. 931-950.

H. R. W. Bailey, "Usefulness and Role of Repeated Strain Testing as an Aid to Engineering Design and Practice," International Conference on Fatigue of Metals, 1956.

I. C. Zener and J. H. Holloman, "Plastic Flow and Rupture of Metals," Transactions of ASM, Vol. 33, 1944, pp. 163-215.

J. W. T. Lankford, R. J. McDonald, and R. L. Carlson, "The Effect of Strain Rate and Temperature on the Stress-Strain Relations of Deep Drawing Steels," Proceedings ASTM, Vol. 56, 1956, p. 704.

K. J. E. Dorn, O. D. Sherby, and T. S. Trogera, "Effect of Strain Rate and Temperature on the Plastic Deformation of High Purity Aluminum," Transactions, ASM, Vol. 49, 1957.

L. J. H. Gross and R. D. Stout, "Plastic Fatigue Behavior of High-Strength Pressure Vessel Steels," The Welding Journal, Vol. 34, Research Supplement 161-S to 166-S, 1955.

M. D. E. Martin, "An Energy Criterion for Low-Cycle Fatigue," ASME, Trans. Ser. D., J. Basic Eng., Vol. 83, December 1961, pp. 565-571.

N. F. G. Crum and F. T. Mavis, "Behavior of Certain Alloys Subjected to Dynamic Loading," ASTM Bulletin No. 231, July 1958, p. 88.

O. E. H. Nickell and W. E. Jacobsen. Factor of Safety Considerations for Aerodynamically Heated Structures Subjected to High Cyclic Stresses, Lockheed Aircraft Corp., Missiles & Space Div., LMSC 2-04-61-1, ASD-TR-61-508, October 1961.